Available online at www.sciencedirect.com
SCIENCE DIRECT
Polymer 47 (2006) 5715–5723
polymer
www.elsevier.com/locate/polymer

Multi-wall carbon nanotubes coated with polyaniline

Elena N. Konyushenko [a], Jaroslav Stejskal [a,*], Miroslava Trchová [a], Jiří Hradil [a], Jana Kovářová [a], Jan Prokeš [b], Miroslav Cieslar [b], Jeong-Yuan Hwang [c,d], Kuei-Hsien Chen [c,d], Irina Sapurina [e]

[a] *Institute of Macromolecular Chemistry, Academy of Sciences of the Czech Republic, 162 06 Prague 6, Czech Republic*
[b] *Charles University Prague, Faculty of Mathematics and Physics, 121 16 Prague 2, Czech Republic*
[c] *Institute of Atomic and Molecular Sciences, Academia Sinica, Taipei, Taiwan*
[d] *Center for Condensed Matter Sciences, National University, Taipei, Taiwan*
[e] *Institute of Macromolecular Compounds, Russian Academy of Sciences, St. Petersburg 199004, Russia*

Received 23 March 2006; received in revised form 23 May 2006; accepted 26 May 2006
Available online 30 June 2006

Abstract

Multi-wall carbon nanotubes (CNT) were coated with protonated polyaniline (PANI) *in situ* during the polymerization of aniline. The content of CNT in the samples was 0–80 wt%. Uniform coating of CNT with PANI was observed with both scanning and transmission electron microscopy. An improvement in the thermal stability of the PANI in the composites was found by thermogravimetric analysis. FTIR and Raman spectra illustrate the presence of PANI in the composites; no interaction between PANI and CNT could be proved. The conductivity of PANI-coated CNT has been compared with the conductivity of the corresponding mixtures of PANI and CNT. At high CNT contents, it is not important if the PANI coating is protonated or not; the conductivity is similar in both cases, and it is determined by the CNT. Polyaniline reduces the contact resistance between the individual nanotubes. A maximum conductivity of 25.4 S cm^{-1} has been found with PANI-coated CNT containing 70 wt% CNT. The wettability measurements show that CNT coated with protonated PANI are hydrophilic, the water contact angle being ~40°, even at 60 wt% CNT in the composite. The specific surface area, determined by nitrogen adsorption, ranges from 20 $m^2 g^{-1}$ for protonated PANI to 56 $m^2 g^{-1}$ for neat CNT. The pore sizes and volumes have been determined by mercury porosimetry. The density measurements indicate that the compressed PANI-coated CNT are more compact compared with compressed mixtures of PANI and CNT. The relaxation and the growth of dimensions of the samples after the release of compression have been noted.

Keywords: Conducting polymer; Carbon nanotubes; Conductivity

1. Introduction

Interest in nanotechnology has greatly stimulated research on carbonaceous materials, such as fullerenes and carbon nanotubes (CNT). Development of nanostructures afforded by conducting polymers, *viz*. polyaniline (PANI) and polypyrrole, proceeds independently and includes the preparation of nanotubes [1–3] and nanofibres [4–7], as well as the coating of various substrates with a thin polymer film [8,9]. The combination of both types of materials on a nano-size level is thus an obvious challenge. This approach is illustrated by the coating of CNT with conducting polymers. The deposition process follows the same principle as the coating of polymer fibres having diameters in micrometre range [10], which is a well-established technique for the preparation of conducting textiles [11].

Both single-wall CNT [12–14] and multi-wall CNT [15–22] have been coated with PANI or polypyrrole *in situ* during the polymerization of the respective monomers. Conducting polymers have been deposited electrochemically in some cases [12,13,17–19,23] but the chemical polymerization of aniline salts using ammonium peroxydisulfate as an oxidant remains

* Corresponding author. Tel.: +420 296 809351; fax: +420 296 809410.
E-mail address: stejskal@imc.cas.cz (J. Stejskal).

0032-3861/$ - see front matter © 2006 Elsevier Ltd. All rights reserved.
doi:10.1016/j.polymer.2006.05.059

the most popular way for the preparation of PANI coatings [14,20,22,24–27].

Carbon nanotubes coated with conducting polymers have been proposed for widely differing applications, including an amperometric biosensor for DNA [18] or choline [19], a sensor for nitrogen oxide [28], an acidity sensor [29], a contact in plastic electronics [30], and in electrorheology [16,31]. PANI nanofibrils have been suggested as candidates for field-emitting applications [32]; the PANI-coated CNT might prove to be an even more promising material. Improvement of the mechanical properties of composites has been mentioned as a frequent goal [21,33–35].

Both carbonaceous materials and conducting polymers [36–38] have been used separately as supports for catalytic systems in the design of fuel cells. Electronic and proton conductivities are keywords in this field [39]. Electrodes combining carbon black or graphite and conducting polymers have been proposed only recently [40–42]. The use of CNT would introduce another dimension, the nanostructure. Such composites have already been used in other energy-conversion applications, such as hydrogen production by electrolysis [43,44] and energy storage in supercapacitors [25].

Having in mind the potential applications of conducting polymers combined with CNT, we have concentrated, in the present paper, on the coating of multi-wall CNT with PANI, using both the conducting protonated form and a non-conducting base [45]. The resulting composite materials have then been characterized with respect to their morphology, thermal stability, conductivity, porosity, wettability, and other characteristics.

2. Experimental

2.1. The coating of CNT with PANI

Multi-wall CNT (L.MWNCTs-2040, Conyuan Biochemical Technology Co., Taipei, Taiwan; specific surface area 40–300 $m^2 g^{-1}$, diameter 20–40 nm, length 5–15 μm) have been coated with PANI *in situ* during the oxidative polymerization of aniline [46] (Fig. 1). Aniline hydrochloride (2.59 g, 20 mmol) was dissolved in ethanol to provide 50 mL of solution, and ammonium peroxydisulfate (5.71 g, 25 mmol) was similarly dissolved in water to yield 50 mL of solution.

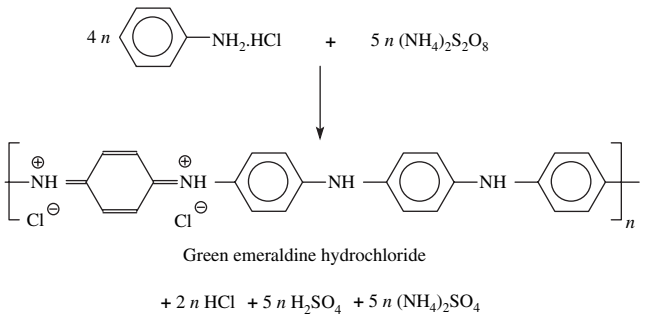

Fig. 1. The oxidation of aniline hydrochloride with ammonium peroxydisulfate yields polyaniline hydrochloride.

The monomer and then the oxidant solutions were added to various portions of CNT to start the polymerization of aniline. The reaction mixture used for the coating of CNT thus contained 0.2 M aniline hydrochloride and 0.25 M ammonium peroxydisulfate in ethanol (50 vol%)–water. The reaction mixture (100 mL) produces 2 g of PANI salt [46]. Composites containing more than 80 wt% CNT could not be prepared in this way because the volume of the reaction mixture was too low to accommodate all the CNT.

The PANI-coated CNT have been collected as solids on a filter, rinsed with 0.2 M hydrochloric acid, then with acetone, and dried at ambient atmosphere. In a portion of the samples, conducting PANI was converted to a non-conducting PANI base by immersion of the composites in excess of 1 M ammonium hydroxide.

Mixtures of protonated PANI or PANI base with CNT for comparative characterization have been prepared by mechanical blending of the components for 10 min with a pestle and mortar. Protonated PANI, for use in blending, has been prepared as above, but in water without ethanol [46].

2.2. Characterization

Electron scanning micrographs have been taken with a JEOL 6400 microscope (Japan), transmission investigations with JEOL JEM 2000FX microscope. Thermogravimetric analysis (TGA) was performed, in air flow (50 $cm^3 min^{-1}$) at a heating rate of 10 °C min^{-1}, with a Perkin Elmer TGA 7 Thermogravimetric Analyzer.

Specific surface area was determined with a Quantasorb apparatus (Quantachrome, USA) using nitrogen as sorbate. Mercury porosimetry was used to characterize the pore size of substrates with a ThermoFinigan PASCAL 440 apparatus in the pore-size range 4 nm–15 μm. The mean pore radius was calculated from the specific surface area and pore volume, assuming the model of cylindrical pores as $r = 2000\,V/S$, where r (nm) is the mean pore radius, V ($cm^3 g^{-1}$) is the pore volume obtained from mercury porosimetry, and S ($m^2 g^{-1}$) is the specific surface area according to the thermal desorption of nitrogen. The porosity was calculated from the pore volumes and true density d of the composite as $p = V/(V + d^{-1})$.

Infrared spectra in the range 400–4000 cm^{-1} were recorded, at 64 scans per spectrum at 2 cm^{-1} resolution, using a fully computerized Thermo Nicolet NEXUS 870 FTIR Spectrometer with DTGS TEC detector. Samples were dispersed in potassium bromide and compressed into pellets. Raman spectra, with the excitation in the visible range of a HeNe 633 nm laser, were collected on a Renishaw inVia Reflex Raman microscope using a 50× objective and 10 s accumulation time. The power was always kept low to avoid destruction of the samples.

The conductivity was measured by a four-point van der Pauw method on pellets compressed at 700 MPa with a manual hydraulic press using a current source SMU Keithley 237 and a Multimeter Keithley 2010 voltmeter with a 2000 SCAN 10-channel scanner card. For non-conducting PANI bases, a two-point method using a Keithley 6517 electrometer was

applied. Before such measurements, circular gold electrodes were deposited on both sides of the pellets.

The density of a composite was evaluated using a Sartorius R160P balance by weighing the pellets in air and immersed in decane. The wettability was assessed with a contact-angle measuring system OCA20, Dataphysic (Germany).

3. Results and discussion

3.1. The course of polymerization

The dispersion of carbonaceous materials in the aqueous medium used for the polymerization of aniline is difficult due to their hydrophobicity. That is why surfactants have often been added to the reaction mixture [15,26,47,48]. In the present case, we have used ethanol (50 vol%) as a component of the reaction medium to avoid this problem. The oxidation of aniline is an exothermic reaction and its course can easily be followed by monitoring the reaction temperature (Fig. 2). A solution of aniline hydrochloride in ethanol containing CNT has been mixed with an aqueous solution of the oxidant. The temperature rose from 20 °C to about 26 °C due to the ethanol–water heat of mixing. After an induction period, the next increase in the temperature is associated with the exothermic polymerization of aniline. The peak temperatures have reached 41–46 °C. This indicates that the conversion of aniline to PANI has practically been complete, as later confirmed by determining the yield of reaction [46], >90%.

The presence of CNT in the reaction mixture significantly accelerates the rate of aniline oxidation. Even 1 wt% of CNT (relative to aniline) reduces the reaction time from 64 min to 17 min by shortening the induction period (Fig. 2). The reaction time decreases on a semi-logarithmic scale about linearly as the content of CNT in the reaction mixture has grown (Fig. 3). A similar accelerating effect has also been reported with single-wall CNT [49].

There are two possible explanations for the observed acceleration of oxidation. The first is based on the assumption of

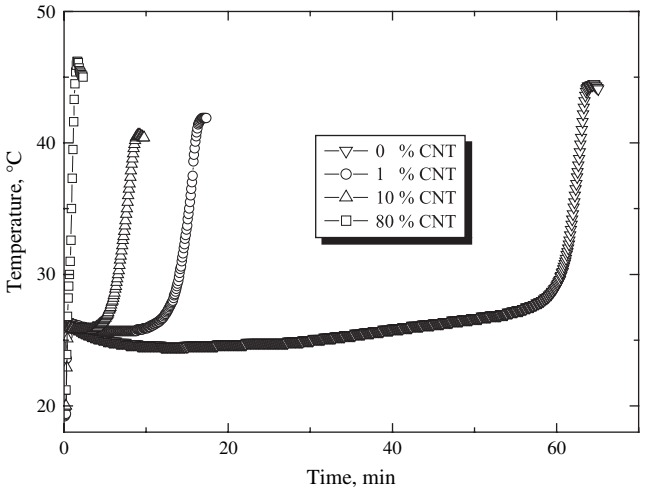

Fig. 2. The course of aniline polymerization in the presence of CNT. The compositions are given as wt% of CNT in the composites.

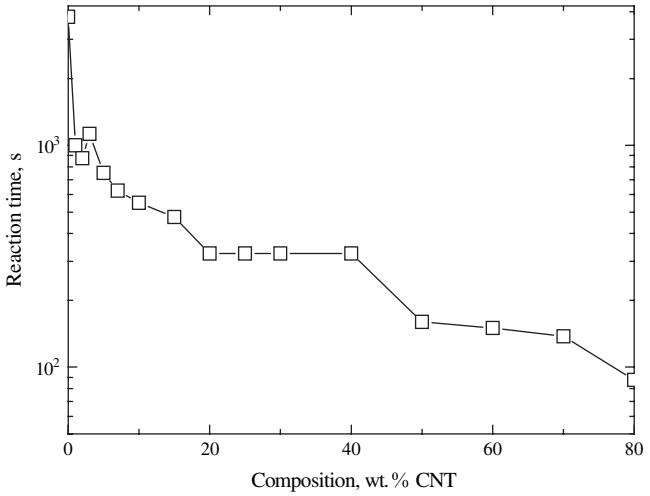

Fig. 3. The rate of composite formation in dependence on the composite composition.

heterogeneous catalysis. The oligomeric aniline intermediates adsorbed at the substrate, having a large surface area, like textile fibres [10] or silica gel [50], start the growth of PANI chains more readily. The CNT have also a high surface area and that is why they could act in a similar manner. Philip et al. [27] proposed the principle of heterogeneous catalysis to be operative in the case of CNT; the oxidation of aniline gets faster at the surface of CNT, resulting in the core–shell morphology of the products (Figs. 4 and 5).

The second explanation is based on the fact that CNT are conducting, *i.e.* they are able to transfer electrons. The oxidation of aniline is a typical redox reaction, in which the electrons are abstracted from aniline molecules and accepted by an oxidant, peroxydisulfate, which converts to sulfate (Fig. 1). In a classical reaction concept, the molecules of aniline and oxidant are expected to meet, and consequently react. It has recently been proposed that conducting materials can mediate the transfer of electrons [51]; CNT can obviously undertake such a role and transfer the electrons between the reductant and oxidant. This means that the aniline molecule at the surface of CNT can exchange electrons, and thus convert to PANI, with any oxidant molecule that is also in contact with CNT, and not only with the oxidant in the close vicinity of the aniline molecule involved. This fact dramatically increases the probability for an aniline molecule to be oxidized to a PANI constitutional unit. The PANI chains growing at the CNT surface are also conducting and thus participate in the electron transfer from the aniline unit that is being added to the PANI chain-end and CNT. That is why the non-conducting textile fibres, after being coated with conducting PANI, also accelerate the polymerization of aniline [10].

3.2. Morphology of PANI-coated CNT

Scanning electron microscopy (SEM) illustrates a uniform coating of CNT with PANI (Fig. 4). The coated CNT become thicker as the amount of deposited PANI increases. The uniform deposition of PANI on the CNT is similarly demonstrated

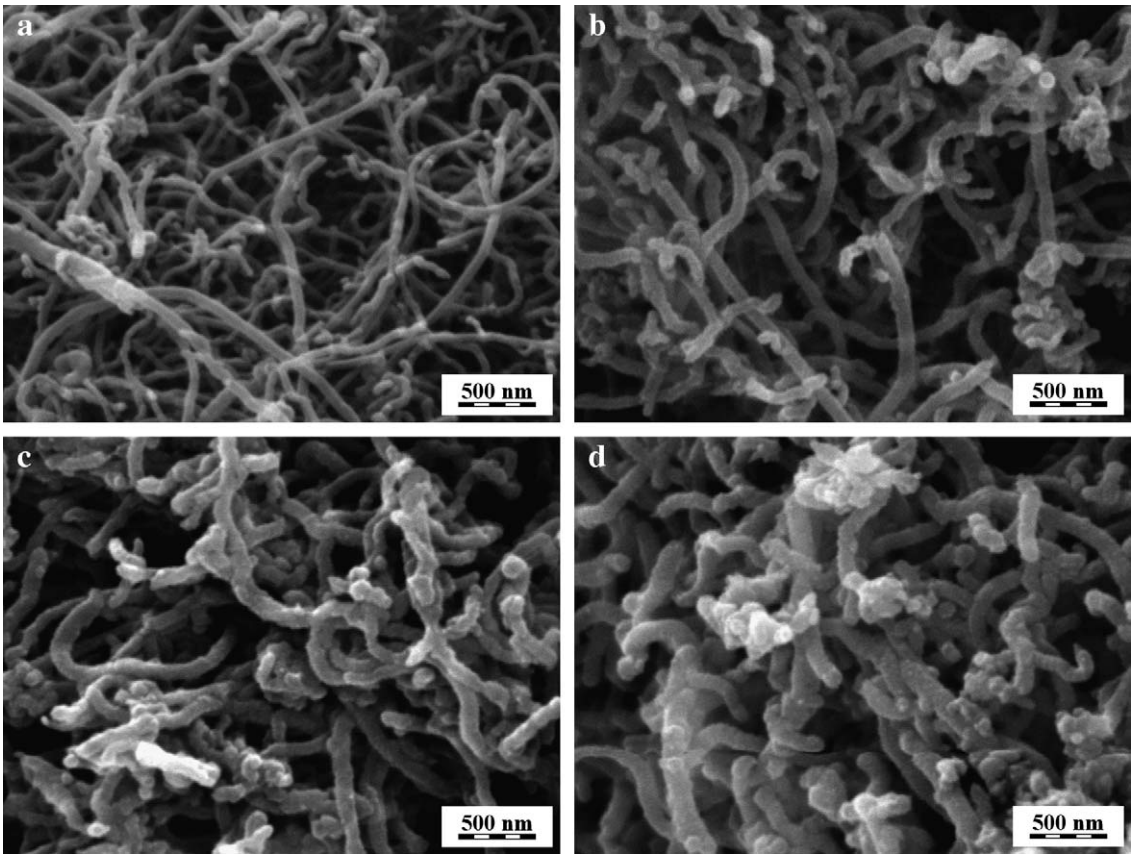

Fig. 4. Original MWCNT (a) and those coated with 50 wt% (b), 70 wt% (c) and 80 wt% PANI (d).

by transmission electron microscopy (TEM), which shows the bilayered structure of coated CNT (Fig. 5). As the internal cavity is well discernible, we conclude that the coating with PANI takes place only at the outer surface of the CNT. The polymerization of aniline inside the CNT is hindered by the restricted access of reactants to the interior of the CNT. The ''droplets'' of PANI on CNT have been observed by Yu et al. [26] at low (1 wt%) PANI loadings while coaxial core–shell agglomerates were produced at higher content (20 wt%) of PANI. Generally, the complete and uniform coating of CNT with a conducting polymer has been reported in the literature [17,23,25,27], in agreement with the present results.

Various modes of functionalization of CNT, *e.g.*, with carboxyl groups [20] or *p*-phenylenediamine [27,52], have been done to improve the interaction of PANI with CNT in the preparation of tubular nanocomposites. The surface of the CNT has also been modified, *e.g.*, by oxidation in nitric acid [13,19,23] or with permanganate [27], to enhance the deposition of conducting polymer. In the present paper, we demonstrate that the deposition of PANI by surface polymerization [50] proceeds well, even on the neat CNT, without any pre-treatment, if the appropriate reaction conditions have been used. This is in accordance with the well-known fact that uniform PANI films are produced by *in situ* polymerization on hydrophobic surfaces [53], and CNT satisfy this condition. The conducting polymer, however, is not covalently bonded to the carbon nanotubes. The aniline oligomers are adsorbed [9] at the surface of CNT and start the growth of polyaniline coating there. Uniform coatings with conducting polymers have thus been obtained by this technique on textiles [11,13,54] and carbon fibres [55] as well as on polymer nanofibres [56]. A good deposition of PANI on CNT is thus not surprising.

3.3. Thermal stability

Thermogravimetric analysis shows the deprotonation of PANI salts in the composites in the temperature region below 200 °C (Fig. 6) and the beginning decomposition of PANI at higher temperatures [57]. Polyaniline protonated with hydrochloric acid has a low thermal stability with respect to deprotonation; the performance could be improved by selecting another acid, like methanesulfonic acid [58]. The thermal stability of PANI in the composite is somewhat better compared with neat PANI (Fig. 6). Neat CNT are stable up to 650 °C and become completely decomposed above 750 °C, in accordance with data reported in the literature [22,26]. The residue of 0.6 wt% confirms that the metal catalyst used in the preparation of CNT has been removed from CNT.

3.4. Raman spectra

Raman spectroscopy is a useful tool for the characterization of carbonaceous materials. The typical G-band (derived from

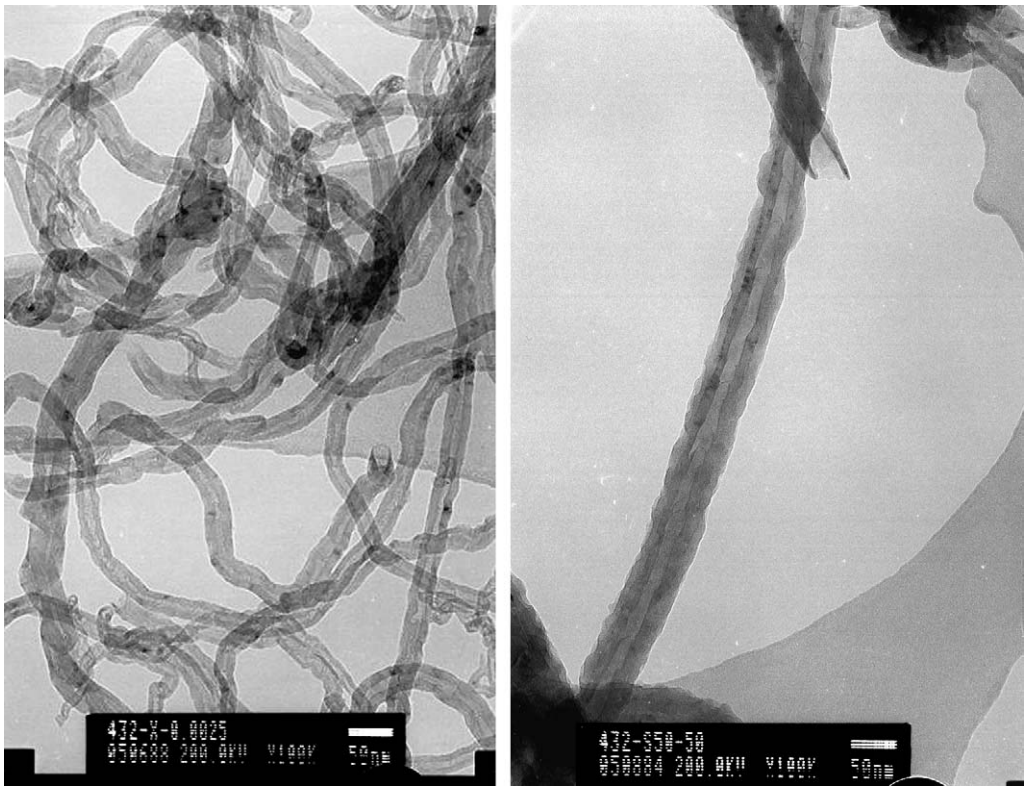

Fig. 5. Original CNT (left) and CNT after coating (right) with polyaniline (50 wt%) at the same magnification.

the graphite-like mode) is situated at 1574 cm^{-1} in the spectrum of neat CNT (Fig. 7). In contrast to the graphite G-band, which exhibits a single Lorentzian peak, the band for CNT has a shoulder extending to higher wavenumbers. Disorder-induced D-band is situated at 1326 cm^{-1} and its second-order harmonic D′-band is found at 2643 cm^{-1}. After the coating of CNT with PANI, the spectrum of this polymer dominates in all samples. This observation confirms that good coating of CNT with PANI has been achieved. The peaks in the spectra are typical of protonated PANI and are located at 1593, 1504, 1330, and 1171 cm^{-1}. Their positions remain practically unchanged for all contents of CNT. We have observed the relative decrease and a shift of the second-order of the disorder-induced band D′ which indicates a less perfect structure for the nanotubes embedded in the polymer [59]. In some cases, Raman spectroscopy showed indications of

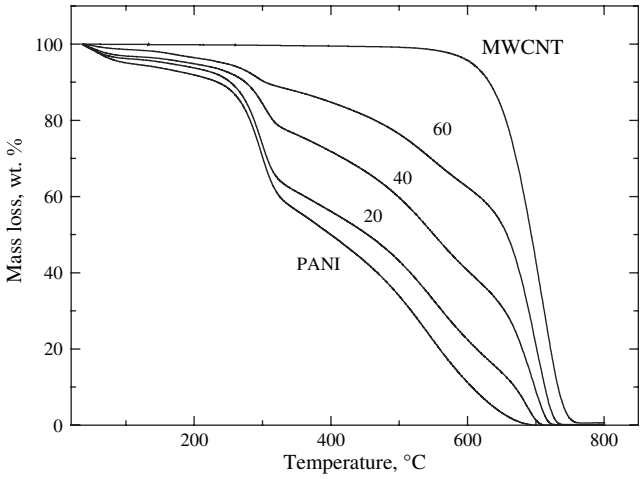

Fig. 6. Thermogravimetric analysis of PANI-coated CNT. The content of CNT (wt%) is given at the individual curves.

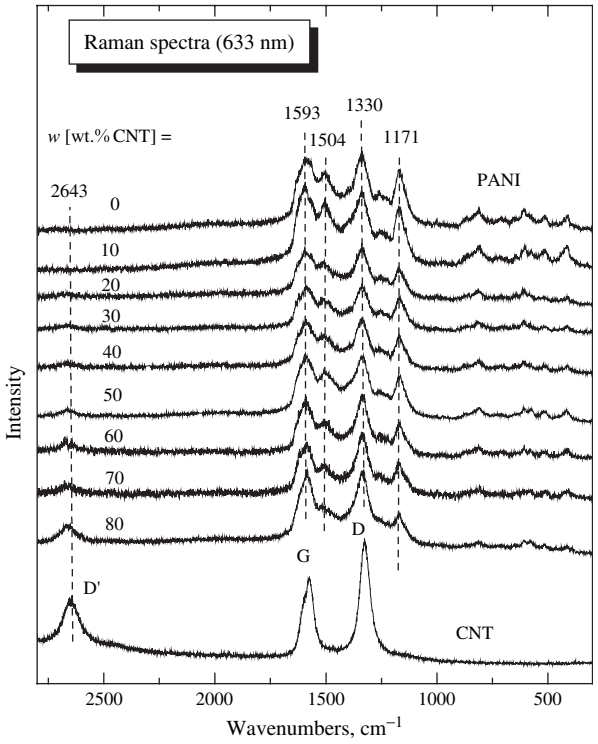

Fig. 7. Raman spectra of carbon nanotubes coated with PANI.

possible interaction between single-wall CNT and conducting polymers [60]. In contrast to polymer-functionalized CNT, where strong effects of the polymer on the Raman signal of CNT have been observed [61,62], no interaction between CNT and PANI could be proved by Raman spectra in the present study.

3.5. FTIR spectra

Raman-active D- and G-bands are inactive in IR spectra because they are forbidden due to the symmetry of the carbon network. That is why the FTIR spectra of neat CNT are featureless (Fig. 8). After coating with PANI, the spectra also reflect the presence of the polymer overlayer. The spectrum of PANI prepared in ethanol–water mixtures is very close to the spectrum of PANI sulfate [8] prepared in an aqueous medium. The main bands are situated at 1560 cm^{-1} (with a shoulder at 1607 cm^{-1}), 1482, 1408, 1301, 1242, 1137, 803, and 575 cm^{-1}. The fact that polymer is protonated in part by sulfate anions is demonstrated by the presence of the peak at 575 cm^{-1}, which is attributed to a stretching vibration in the sulfate anion [63].

Some authors have reported that an interaction between multi-wall CNT and conducting polymers manifested itself by the shifts in FTIR spectra [25,26,48], while no interaction between CNT and PANI was found by Karim et al. [13]. Baibarac et al. [59] showed that composites of PANI and single-wall CNT were different when they had been prepared by adding dispersed single-wall CNT to the polymer solutions or when they have been prepared by chemical polymerization

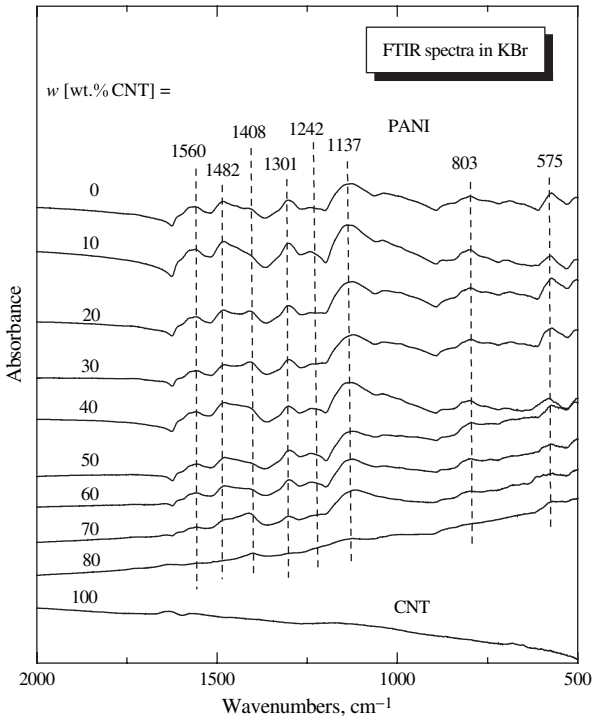

Fig. 8. FTIR spectra of carbon nanotubes coated with PANI.

of aniline in the presence of single-wall CNT. In the present case, the spectrum of PANI exhibits changes in the intensity in the region at about 1400 cm^{-1} probably corresponding to the hydrogen-bonded C–N^{+} stretching vibration [64] and at about 1242 cm^{-1}, which is interpreted as a C–$N^{+\bullet}$ stretching vibration in the polaron structure of PANI [65]. The prominent 1137 cm^{-1} band assigned to a vibration mode of the –$NH^{\bullet+}$– structure [66] exhibits a slight variation in its shape. Baibarac et al. [59] described the intensity increase of this band to charge transfer between the PANI and CNT. The electronic interaction between a semiconductor, like a conducting polymer, and carbon, like graphite or CNT, has also been suggested in the literature [67]. The question whether the molecular interaction between PANI and CNT takes place cannot be answered on the basis of present FTIR spectra.

3.6. Conductivity of PANI–CNT mixtures

Four series of samples have been prepared for the conductivity measurements: mixtures of PANI with CNT and PANI-coated CNT, PANI being either in the conducting protonated state or as a non-conducting PANI base.

The mixtures of protonated PANI with CNT show simple behaviour, the conductivity gradually increasing from 0.9 S cm^{-1} for PANI hydrochloride to a maximum at 7.7 S cm^{-1} for a mixture with 70 wt% CNT (Fig. 9a). The neat CNT could not be compressed to a pellet, as is necessary for conductivity measurement.

The mixtures of PANI base with CNT exhibit typical percolation behaviour (Fig. 9a). The conductivity of PANI base suddenly increases as the percolation threshold, located at 4 wt% of CNT, is passed. At this concentration of the conducting component, the first conducting pathways are produced in the composite. The percolation limit is lower than that expected for spherical particles ($\sim$16 vol%) and reflects the nanotubular character of CNT in the mixture. On the other hand, the percolation limit was estimated to be between 15 and 20 wt% CNT in a similar composite of CNT with polypyrrole [68]. The different degrees of dispersion of the CNT in the polymer matrix may be responsible for the observed difference.

3.7. Conductivity of PANI-coated CNT

The dependence of conductivity on CNT content for CNT coated with the conducting form of PANI is similar to that of corresponding mixtures (Fig. 9b). At low fractions of CNT, the conductivity is determined by the PANI as the main component. It increases moderately from 0.42 S cm^{-1} for neat PANI with increasing CNT content. The decrease in the contact resistance of CNT afforded by a PANI coating [69] results in the maximum composite conductivity of 25.4 S cm^{-1} at 70 wt% CNT. This is a much higher conductivity than that of the order of 10^{-1} S cm^{-1} reported for similar composites by some authors [20,48], and comparable with other reported results [24,47,70] that are of the order of 10^{0}–10^{1} S cm^{-1}. At higher CNT content, the conductivity

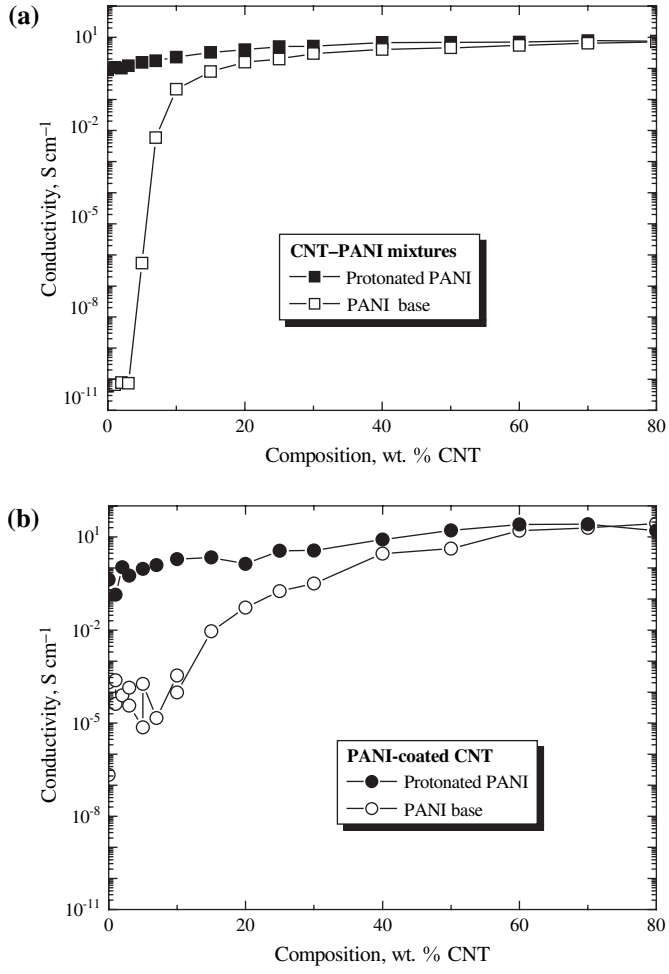

Fig. 9. The conductivity of carbon nanotubes mixed (a) or coated (b) with protonated PANI (filled symbols) and PANI base (open symbols).

was reduced; the amount of PANI is not sufficient to provide good contact between the CNT and the resistance between the CNT increases. Reduction of the thickness of the PANI coating could possibly be the way to increase the composite conductivity by introducing the tunneling mechanism of conduction.

The increase in the conductivity of CNT coated with PANI base with increasing content of CNT is slower (Fig. 9b), compared with the corresponding mixtures (Fig. 9a). At low concentrations of CNT, the direct electrical contact between CNT is prevented by the surface coating with a non-conducting PANI base and the percolation threshold is thus practically not distinguishable. Yet, the coating with PANI base seems to reduce the contact resistance between CNT. The resulting conductivity of CNT coated with PANI base thus reaches 19.6 S cm^{-1} at 70 wt% CNT. The conductivity is thus comparable with that of the CNT coated with protonated PANI. We are obviously dealing with interfacial phenomena between the CNT separated with a thin coating of PANI. A non-conducting PANI base is not a true insulator, but it can probably mediate the charge-carrier transfer over short distances between the neighboring CNT, similarly to the protonated conducting form.

3.8. Contact-angle measurements

The contact angle of water on ''standard'' PANI hydrochloride is [71] 49°. When PANI has been prepared in ethanol (50 vol%)–water mixture, the contact angle was 43°. The enhanced wettability is possibly due to the sulfonation of aromatic rings under these reaction conditions. The contact angles of CNT coated with protonated PANI are about ~40° (Fig. 10) up to 60 wt% CNT in the composite. The composite is thus hydrophilic and behaves as a neat PANI. This is not surprising considering the core–shell morphology of the composite (Fig. 5). At higher contents of CNT, the contact angles could not be measured. The water droplet penetrated into the composite, possibly as a result of higher porosity. This means that the contact angle of neat CNT could not be determined but we expect that, by analogy with graphite, they are more hydrophobic; the contact angle of water on graphite is 79°. The mixtures of PANI with CNT behave differently. Even a small fraction of CNT in PANI increases the contact angle towards the level expected for neat CNT (Fig. 10). Despite the hydrophobic behaviour, above 10 wt% CNT, water penetrated the samples, and contact angles again could not be determined.

3.9. Surface area and porosity

Basic properties of the porous structure of CNT coated with PANI were determined by standard methods, such as mercury porosimetry and thermal desorption of nitrogen (Table 1). The specific surface area of PANI, 20.2 $m^2 g^{-1}$, is lower than that of PANI prepared by, *e.g.*, mechanochemical synthesis [72], 69.7 $m^2 g^{-1}$. The surface areas of PANI-coated CNT are in the range from 12 to 55 $m^2 g^{-1}$. They are proportional to the micropore content, *i.e.* the pore area where the adsorption interactions occur. The highest values represent a good sorption ability of such materials.

Mercury porosimetry allows us to determine the pore volume and pore-size distribution. The pore volumes are in range from 0.4 to 2.5 $cm^3 g^{-1}$ (Table 1). The mean pore radii

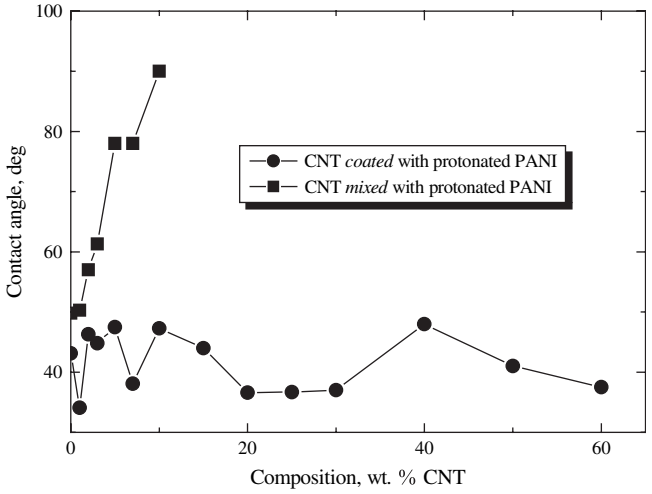

Fig. 10. Water contact angles on PANI-coated CNT and on the mixtures of protonated PANI with CNT.

Table 1
Porosity parameters of PANI-coated CNT

CNT (wt%)	Pore volume ($cm^3\ g^{-1}$)	Specific surface area ($m^2\ g^{-1}$)	Porosity (%)	Mean pore radius (nm)	Most frequent radius (nm)
0	0.42	20.2	30	432	35
10	0.87	48.8	47	36	61
20	0.58	19.3	37	61	82
30	0.63	12.9	39	97	71
40	1.04	50.0	51	42	56
50	0.99	34.9	50	57	60
60	1.65	51.9	62	64	47
70	1.41	31.0	59	91	40
80	0.92	20.6	48	89	53
100	2.54	56.5	72	90	20

calculated from the specific surface area and pore volume are in an interval from 35 to 96 nm. Such pores are in the area of mesopores. Pore-size distribution curves have two maxima, as illustrated on the PANI-coated CNT (20 wt%) (Fig. 11). The first, at about 750 nm, reflects the interstices between the nanotubes, and the second, at 65 nm, represents the actual pores. The porosity was calculated from pore volume values and the true density of the composite. Values from 30 to 72% are common for a wide range of adsorbents.

3.10. Density

The density of "standard" PANI hydrochloride is [46] 1.33 $g\,cm^{-3}$ and the density of PANI base 1.24 $g\,cm^{-3}$. The density of materials containing the protonated form of PANI was always higher than with the composites of PANI base, as expected (Fig. 12). This applies both to mixtures of PANI with CNT and to PANI-coated CNT. The dependence of density on the content of CNT, however, is different for these two sample sets. The density of PANI-coated CNT increases with increasing CNT content, and the density of neat CNT can be estimated by extrapolation as 1.9 $g\,cm^{-3}$. The density of mixtures, on the contrary, has a decreasing trend. In the latter case,

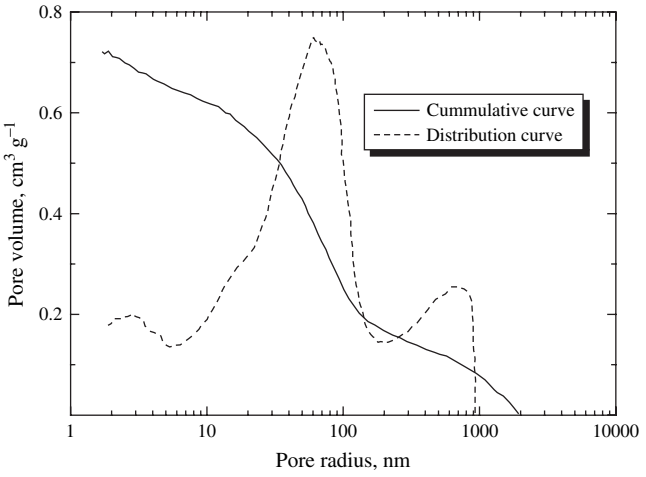

Fig. 11. Example of the pore-size distribution obtained by mercury porosimetry for the PANI-coated CNT (20 wt%).

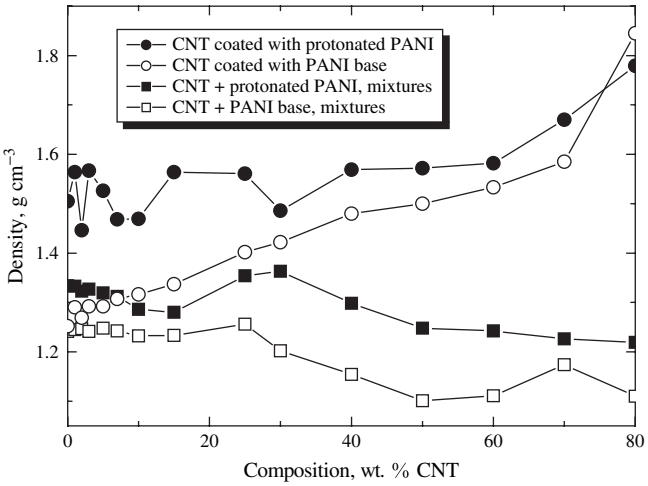

Fig. 12. Densities of CNT coated (circles) or mixed (squares) with PANI in the conducting protonated state (filled symbols) or as a non-conducting PANI base (open symbols).

the low apparent density has to reflect the porous structure of composites. We have indeed observed that the dimensions of the pellets used for the density measurements increase during a number of hours after the compression of the material at 700 MPa. The relaxation, manifested as an increase in pellet diameter, has often exceeded 10%. Such a process is expected to be associated with the formation of macropores within the sample.

4. Conclusions

The presence of CNT in the reaction mixture used for the oxidation of aniline dramatically increases the rate of PANI formation. Electron microscopy shows that CNT become coated with PANI during the *in situ* polymerization of aniline. The coating is uniform and its thickness increases with increasing content of PANI in the composite. The thermal stability of PANI in the composites with CNT is better than the stability of neat PANI. All composites completely disintegrate after heating to 700–750 °C. FTIR and Raman spectra confirm the presence of PANI in the samples; interaction between the two components, PANI and CNT, could not be proved.

The mixtures of CNT with PANI base show typical percolation behaviour, while the dependence of the conductivity of PANI base-coated CNT on the content of CNT is smooth. At high content of CNT, it is not important whether the coating is conducting (with protonated PANI) or non-conducting (with PANI base). The conductivity is controlled by the CNT. The highest conductivity, 25.4 $S\,cm^{-1}$, has been recorded for CNT (70 wt%) coated with protonated PANI.

CNT coated with protonated PANI are hydrophilic, like neat PANI, up to 60 wt% CNT in the sample, the contact angle for water being ~40°. The samples with higher content of CNT could not be characterized because the water droplet penetrated into the sample. Mixtures of PANI and CNT behave quite differently and are more hydrophobic than PANI-coated CNT.

The specific surface areas of PANI-coated CNT were between $20\,m^2\,g^{-1}$ for protonated PANI and $56\,m^2\,g^{-1}$ for neat CNT, the pore volume increased from $0.42\,cm^3\,g^{-1}$ for PANI to $2.54\,cm^3\,g^{-1}$ for CNT. While the density of PANI-coated CNT increases with increasing content of CNT in the samples, this parameter decreases in mixtures of PANI with CNT. The compressed PANI-coated CNT are thus more compact compared with the mixtures containing a similar fraction of CNT, which are porous. All these parameters indicate that PANI-coated CNT might constitute useful materials for various applications, *e.g.*, in fuel cells.

Acknowledgments

The authors thank the Academia Sinica, Taipei, Taiwan, for the support of Czech–Taiwanese cooperation, the Grant Agency of the Academy of Sciences of the Czech Republic (A4050313 and A400500504), the Ministry of Education, Youth, and Sports of the Czech Republic (MSM 0021620834 and ME 847), and the Federal Agency for the Science and Innovations (N2005-RI-12.0/004/028) for financial support.

References

[1] Zhang LJ, Wan MX. Nanotechnology 2002;13:750.
[2] Zhang Z, Wei Z, Zhang L, Wan M. Acta Mater 2005;53:1373.
[3] Konyushenko EN, Stejskal J, Šeděnková I, Trchová M, Sapurina I, Cieslar M, et al. Polym Int 2006;55:31.
[4] Huang J, Kaner RB. Angew Chem Int Ed 2004;43:5817.
[5] Nickels P, Dittmer WU, Beyer S, Kotthaous JP, Simmel FC. Nanotechnology 2004;15:1524.
[6] Ma Y, Zhang J, He H. J Am Chem Soc 2004;126:7097.
[7] Kim B-K, Kim YH, Won K, Chang H, Choi Y, Kong K-J, et al. Nanotechnology 2005;16:1177.
[8] Geng Y, Li J, Sun Z, Jing X, Wang F. Synth Met 1998;96:1.
[9] Stejskal J, Sapurina I. Pure Appl Chem 2005;77:815.
[10] Tzou K, Gregory RV. Synth Met 1992;47:267.
[11] Martin CR. Handbook of conducting polymers. In: Skotheim TA, Elsenbaumer RL, Reynolds JR, editors. 2nd ed. New York: M Dekker; 1998. p. 409–21.
[12] Vivekchand SRC, Sudheendra L, Sandeep M, Govindaraj A, Rao CNR. J Nanosci Nanotechnol 2002;2:631.
[13] Karim RM, Lee CJ, Park Y-T, Lee MS. Synth Met 2005;151:131.
[14] Ham HT, Choi YS, Jeong N, Chung IJ. Polymer 2005;46:6308.
[15] Wu M, Snook GA, Gupta V, Shaffer M, Fray DJ, Chen GZ. J Mater Chem 2005;15:2297.
[16] Choi HJ, Park SJ, Kim ST, Jhon MS. Diam Relat Mater 2005;14:766.
[17] Guo D-J, Li H-L. J Solid State Electrochem 2005;9:445.
[18] Cheng G, Zhao J, Tu Y, He P, Fang Y. Anal Chim Acta 2005;533:11.
[19] Qu F, Yang M, Jiang J, Shen G, Yu R. Anal Biochem 2005;344:108.
[20] Zhang X, Zhang J, Liu Z. Appl Phys A 2005;80:1813.
[21] Wu T-M, Lin Y-W, Liao C-S. Carbon 2005;43:734.
[22] Sainz R, Benito AM, Martínez MT, Galindo JF, Sotres J, Baró AM, et al. Adv Mater 2005;17:278.
[23] Han G, Yuan J, Shi G, Wei F. Thin Solid Films 2005;474:64.
[24] Cochet M, Maser WK, Benito AM, Callejas AM, Martínez MT, Benoit J-M, et al. Chem Commun 2001;1450.
[25] Deng MG, Yang BC, Hu YD. J Mater Sci 2005;40:5021.
[26] Yu Y, Che B, Si Z, Li L, Chen W, Xue G. Synth Met 2005;150:271.
[27] Philip B, Xie J, Abraham JK, Varadan VK. Polym Bull 2005;53:127.
[28] An KH, Jeong SY, Hwang HR, Lee YH. Adv Mater 2004;16:1005.
[29] Kaempgen M, Roth S. J Electroanal Chem 2006;586:72.
[30] Lefenfeld M, Blanchet G, Rogers JA. Adv Mater 2003;15:1188.
[31] Park SJ, Park SY, Cho MS, Choi HJ, Joo J. Mol Cryst Liq Cryst 2004;425:21.
[32] Wang C, Wang Z, Li M, Li H. Chem Phys Lett 2001;341:431.
[33] Wang M, Pramoda KP, Goh SH. Polymer 2005;46:11510.
[34] Chae HG, Sreekumar TV, Uchida T, Kumar S. Polymer 2005;46:10925.
[35] Zeng H, Gao C, Wang Y, Watts PCP, Kong H, Cui X, et al. Polymer 2006;47:113.
[36] Drelinkiewicz A, Waksmundzka-Góra A, Makowski W, Stejskal J. Catal Commun 2005;6:347.
[37] Samant PV, Rangel CM, Romwero MH, Fernandes JB, Figueiredo JL. J Power Sources 2005;151:79.
[38] Holzhauser P, Bouzek K, Bastl Z. Synth Met 2005;155:501.
[39] Treptow F, Jungbauer A, Hellgardt K. J Membr Sci 2006;270:115.
[40] Rajesh B, Thampi KR, Bonard JM, Mathieu HJ, Xanthopoulos N, Viswanathan B. Electrochem Solid State Lett 2004;7:A404.
[41] Wu Y, Li L, Jing-Hong L, Xu BQ. Carbon 2005;43:2579.
[42] Park JC, Kim JS, Jung DH. Macromol Res 2002;10:181.
[43] Navarro-Flores E, Omanovic S. J Mol Catal A Chem 2005;242:182.
[44] Damian A, Omanovic S. J Power Sources, in press.
[45] Stejskal J, Kratochvíl P, Jenkins AD. Polymer 1996;37:367.
[46] Stejskal J, Gilbert RG. Pure Appl Chem 2002;74:857.
[47] Zhang X, Zhang J, Wang R, Liu Z. Carbon 2004;42:1455.
[48] Yu Y, Ouyang C, Si Z, Chen W, Wang Z, Xue G. J Polym Sci Part A Polym Chem 2005;43:6105.
[49] Zhou Y, He B, Li H. J Electrochem Soc 2004;151:A1052.
[50] Stejskal J, Trchová M, Fedorova S, Sapurina I. Langmuir 2003;19:3018.
[51] Kocherginsky NM, Lei W, Wang Z. J Phys Chem A 2005;109:4010.
[52] Philip B, Xie J, Abraham JK, Varadan VK. Smart Mater Struct 2004; 13:N105.
[53] Huang Z, Wang P-C, MacDiarmid AG, Whitesides G. Langmuir 1997;13:6480.
[54] Varesano A, Dall'Acqua L, Tonin C. Polym Degrad Stab 2005;89:125.
[55] Paligová M, Vilčáková J, Sáha P, Křesálek V, Stejskal J, Quadrat O. Physica A 2004;335:421.
[56] Dong H, Prasad S, Nayme V, Wayne Jr EJ. Chem Mater 2004;16:371.
[57] Trchová M, Matějka P, Brodinová J, Kalendová A, Prokeš J, Stejskal J. Polym Degrad Stab 2006;91:114.
[58] Prokeš J, Stejskal J. Polym Degrad Stab 2004;86:187.
[59] Baibarac M, Baltog I, Lefrant S, Meveller JY, Chauver G. Chem Mater 2003;15:4149.
[60] Ferrer-Anglada N, Kaempgen M, Skákalová V, Dettlaf-Weglikowska U, Roth S. Diam Relat Mater 2004;13:256.
[61] Gao C, Jin YZ, Kong H, Whitby RLD, Acquah SFA, Chen GY, et al. J Phys Chem B 2005;109:11925.
[62] Zeng H, Gao C, Yan D. Adv Funct Mater 2006;16:812.
[63] Socrates G. Infrared and Raman characteristic group frequencies. New York: Wiley; 2001. p. 78–167.
[64] Holly S, Sohár P. Absorption spectra in the infrared region – theoretical and technical introduction. Budapest: Akadémiai Kiadó; 1975.
[65] Quillard S, Louarn G, Buisson JP, Boyer M, Lapkowski M, Pron A, et al. Synth Met 1997;84:805.
[66] Chiang JC, MacDiarmid AG. Synth Met 1986;13:193.
[67] Tchmutin IA, Ponomarenko AT, Krinichnaya EP, Kozub GI, Efimov ON. Carbon 2003;41:1391.
[68] Long Y, Chen Z, Zhang X, Zhang J, Liu Z. J Phys D Appl Phys 2004; 37:1965.
[69] Long Y, Zhang L, Ma Y, Chen Z, Wang N, Zhang Z, et al. Macromol Rapid Commun 2003;24:938.
[70] Feng W, Bai XD, Lian YQ, Liang J, Wang XG, Yoshino K. Carbon 2003; 41:1551.
[71] Shishkanova TV, Sapurina I, Stejskal J, Král V, Volf R. Anal Chim Acta 2005;553:160.
[72] Huang JX, Moore JA, Acquaye JH, Kaner RB. Macromolecules 2005; 38:317.